

Sputtering of high entropy alloys thin films: An overview

S.S. Oladijo^a, E.T. Akinlabi^b, F.M. Mwema^{a,b}, T.C. Jen^{a*} and O.P. Oladijo^{a,c}

^aDepartment of Mechanical Engineering Science, University of Johannesburg, South Africa

^bDepartment of Mechanical & Construction Engineering, Northumbria University, United Kingdom

^cDepartment of Chemical, Materials, and Metallurgical Engineering, Botswana International University of Science and Technology, Botswana

ARTICLE INFO

Article history:

Received 22 May 2023

Accepted 9 September 2023

Available online
9 September 2023

Keywords:

High entropy alloys

HEAs applications

HEAs properties

Thin films

Sputtering

ABSTRACT

For the past 19 years, high entropy alloys (denoted as HEAs) have piqued the interest of many researchers due to their unique properties. Sputtering High Entropy Alloys on bulk materials, on the other hand, have been widely utilized due to their low cost of manufacture. This paper reviews the most recent trends and advancements in sputtered HEA coatings, thin film research, and development. Firstly, HEA coating and thin films were introduced. Then, a look at sputtering technologies and procedures is presented, followed by a summary of recent research on sputtered HEA thin films, properties, and applications. From reviewed literature, it can be deduced that HEAs that include the full nitride element have greater mechanical and elastic properties, and HEAs generally have the potential for structural, industrial, biomedical, and energy applications. Finally, it is suggested that new stable HEA films and coating research initiatives with various materials be undertaken to widen its applications.

© 2024 Growing Science Ltd. All rights reserved.

1. Introduction

An alloy can be defined as one or more elements of minor quantity additions to the primary metal in order to modify its physical, chemical, and mechanical properties in a promising way (Praveen & Kim, 2018). In 3000 BC, bronze Sn and Cu alloys were the first set of alloys to be accidentally discovered which played a role that is very significant in the physical metallurgy process. Since then, strategies on the development of alloy have focused on one or two principal elements, for example in over 1000 years ago, a few percentages of the weight of copper were added to the pure silver to form sterling silver for coinage and jewelries because silver is too soft. Furthermore, with few exceptions, the basic strategy of adding alloys with a secondary element of a small relative amount to the primary element remains unchanged and reflected after their principal constituent's name such as titanium alloy, ferrous alloy, nickel alloy, aluminum alloy, and so on. However, this method limits the number of alloys that can be coupled, resulting in the discovery of new ways to dramatically expand the compositional space to be explored, such as increasing the material properties (George et al., 2019). Until 2004, when two groups of researchers published two seminar papers outlining an intriguing justification for a novel alloy class incorporating many elements, dubbed "High Entropy Alloys" (HEA) (Cantor et al., 2004; Kawagishi et al., 2009; George et al., 2019; Yeh et al., 2004).

In the manufacturing and material focus for super alloys, HEA is one of the newest fields. Because it reveals intricate HEA properties, some researchers and scientists have referred to them as high strength alloys (HSAs), complex concentrated alloys (CCAs), composite complex alloys (CCAs), or multicomponent alloys (MCAs) (Kishore Reddy et al., 2019). The term "HEA" refers to a multicomponent system having at least five primary metallic components that are close to or equiatomic in composition and have an equal atomic concentration (Arif et al., 2022), as can be seen in Figure 1. HEAs often crystallizes into a simple phase crystal structure like the body-centered cubic (BCC) or cubic close-packed (CCP) structure (Zhao et al.,

* Corresponding author.

E-mail addresses: tjen@uj.ac.za (T.C. Jen)

ISSN 2291-8752 (Online) - ISSN 2291-8744 (Print)

© 2024 Growing Science Ltd. All rights reserved.

doi: 10.5267/j.esm.2023.9.002

2013; Senkov et al., 2010; Zendejas Medina et al., 2020). Furthermore, HEAs consists of a concentration of between 5-35 atom weight % for each component element (Kemény et al., 2021) and exhibit a variety of desirable properties, such as preference for single-phase solid solutions, single crystal structure, lattice distortions, slow kinetics, and properties superior to constituent materials (Oses et al., 2020). Samaei et al. (2015), reviewed the mechanical and microstructural properties and behavior of HEA materials. HEA is also representing the new paradigm in the development of material in the terms of providing good formability, unique magnetic and electrical properties, ultra-high-strength, high thermal stability, and excellent fracture toughness (Ayyagari, Gwalani, et al., 2018). Furthermore, the HEA possess exceptional bulk properties such as showing excellent mechanical properties at cryogenic as well as elevated temperatures, superior surface oxidation, and irradiation damage resistance, and also exceptional tolerance to damage the material surface via corrosion, wear, tribocorrosion, and erosion (Ayyagari, Barthelemy, et al., 2018; Ayyagari, Gwalani, et al., 2018; Diao et al., 2017; Lei et al., 2018; Miracle, 2019; Qiu et al., 2017). These high entropy alloys characteristics make it qualify as a potential candidate to meet the requirements in extreme applications such as aerospace, turbine, nuclear industries, and so on (Liao et al., 2017a). However, from the application viewpoint in cutting inserts, extrusion dies, the metal powder cost used in the production of the bulk HEA is very expensive. Therefore, coating HEA on a low-cost substrate can effectively be considered a viable economic way to drastically reduce the cost of production for industrial application and counter the limitations of the coatings that are employed in harsh environments, like radiation resistance, cutting tools, aerospace, and extrusion dies.

Generally, entropy alloys can be divided into three (3) different types such as (1) “Low entropy alloy (LEA) $\Delta S_{\text{conf}} < 1R$ which contain one or two elements and can also be called conventional alloy”. (2) “Medium entropy alloy (MEA) $1R \leq \Delta S_{\text{conf}} \leq 1.5R$ which contain two to four principal elements” and (3) “High entropy alloy (HEA) $1R \leq \Delta S_{\text{conf}} \leq 1.5R$ which contain at least four principal elements”. Furthermore, HEAs coating can be divided into three based on the types of elements they contain (Aliyu & Srivastava, 2019; Deng et al., 2021; Chen et al., 2019; Wu et al., 2015), as explained below.

- i) The HEA-based metallic coatings: this include refractory (a collection of metallic elements that are incredibly resistant to wear and heat) high-entropy (RHEA) coatings, which comprise elements with significantly higher melting temperatures (T_m), such as Mo, Nb, Hf, V, W, Zr, etc., as well as transition metal-based HEA coatings, which are composed of transition elements like Co, Fe, Cu, Al, Cr, Ti, Mn, Ni, and V. while the primary materials used to create HEAs are Cr, Ni, Co, and Fe. (M. Zhang et al., 2017b). The example of this coating can be, HfNbTaZr, MoNbTaW, CrNbVZr, CrMoNbTa, CoCrCuFeNi and CrMnFeCoNi series.
- ii) HEA based ceramic coatings: HEAs are combined with boron, oxygen, and other negatively charged elements to create ionic and covalent bonded coatings. These coatings contain strong carbide, boride or nitride forming substances such as Cr, Al, Zr, Nb, Ti, Si, etc. Examples are ZrTaNbTi, HfZrTiTaNb, TiZrNbAlYCr, AlCrMoSiTi, etc.
- iii) HEA based composite coatings: this consist of the element that acts as binder or matrix with reinforcement of hard ceramics such as TiN, NbC, TiC, etc., and reinforcement of lightweight alloys such as Mg, Al and so on. Examples of these coatings are TiN/CoCr₂FeNiTi, NbC/AlCoCrFeNi, Al–CrMnFeCoMoW composite coating and so on.

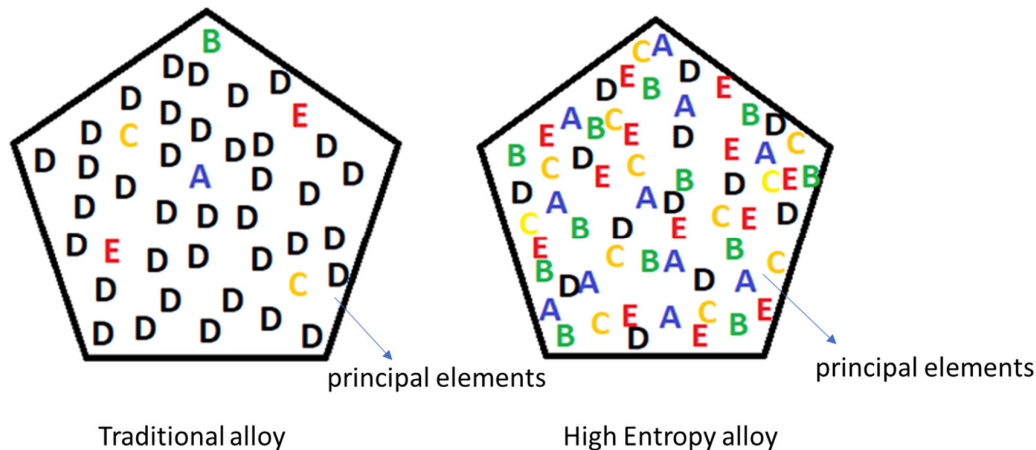


Fig. 1. HEAs and traditional alloy's schematic atomic structure diagram

2. High Entropy Alloy (HEA) Thin films

Many deposition techniques can be used in the deposition of high entropy alloys such as spraying, electro-spark deposition, electrochemical deposition, laser cladding, and sputtering deposition techniques (Alvi et al., 2020a; Chen et al., 2020; Khan et al., 2019a; Zhang et al., 2017a; Sharma, 2021; Yalamanchili et al., 2017; Yoosefan et al., 2020). However, the sputtering deposition process has numerous advantages over other deposition processes such as the ability to vary the deposition process

parameters, energetics species used to enable better coating stoichiometry control, and the and ability to achieve a lower film growth temperature, which is facilitated via the energy added to the growing film via the bombardment of ion. Additionally, the film microstructure's, orientation, and varied grain size which govern the properties of the films can be achieved by varying the sputtering process parameter. Furthermore, the sputtering deposition technique is a physical vapor deposition variant and it is a prominent and favourable deposition technique for surface material deposition due to its outstanding advantages such as its apparatus, excellent adhesion, high deposition rate, low deposition temperature, and can be easily operated (Abegunde et al., 2019; Oladijo et al., 2021; Market & Electronics, 2010; Oluwatosin Abegunde et al., 2019; Li et al., 2018).

Sputtering deposition technique can be used to coat HEAs thin layer in three different ways.

- i) Sputtered HEA films can be deposited directly from prepared HEA target. This process provides good control over the sputtered film stoichiometry, making it a common method for producing sputtered HEA films. Because the target surface composition equilibrates following the pre-sputter stage and, the deposited films can easily match the original target alloy's stoichiometry, even if the constituent elements have varying sputtering yields. Furthermore, the energetic atom can extinguish condensation in thin films quickly (109 K/s), thereby decreasing concentration changes (Cheng et al., 2011; Feng et al., 2020; Li et al., 2018; Liao et al., 2017b; Khan et al., 2020; Xing et al., 2019). The target utilized in this magnetron sputtering is made of solid material and takes the form of a tube, plate, or disc (as shown in Figure 2). The majority of these solid targets are fabricated to solid blocks of material, and their production is based on well-known metallurgical processes like casting, hot isostatic pressing, and arc melting, among others.
- ii) Co-deposition with numerous mosaic and metal targets can be used to sputter HEA films. By avoiding the time-consuming target preparation step, this approach permits sputtering of HEA thin films in a variety of chemical combinations, The relative surface fraction of each element and the target power on a particular target can be changed to influence stoichiometry. Changing the deposition conditions, however, makes it more difficult to get a desired film composition (Feng et al., 2013; Braic et al., 2013; Lin et al., 2012).
- iii) Powder targets (as shown in Fig. 2) can be used to sputter HEAs films. This technique entails selecting the needed metallic powders, weighing, mixing, and ultimately cold pressing the powder combination to make the powder target. Because the number of magnetrons is reduced to one, this method is quick and versatile, and the target composition can be altered simply by modifying the weight fractions of the different powders. One downside to this approach is that the powder must be thoroughly mixed in order for the target to have a uniform composition (Braeckman et al., 2015a; Braeckman et al., 2015b; Liang et al., 2020; Mwema et al., 2020; Schwarz et al., 2021; Li et al., 2018). Hence, the sputtering parameters play a significant role in determining the film quality. Also, sputtered powder targets, according to Depla (Depla, 2021) are a fascinating laboratory method for examining material characteristics because they enable flexible investigation of the effects of material chemical composition attributes without interrupting the experimental setup.

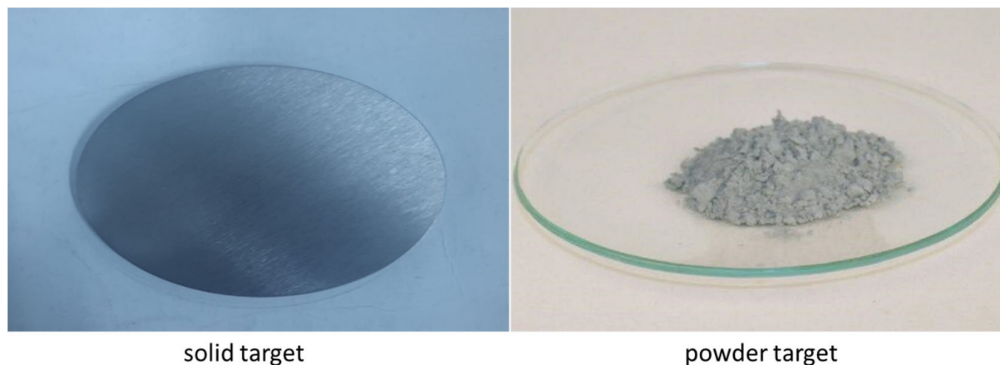


Fig. 2. Disc solid target and powder target diagram

The goal of HEAs thin film researchers is to create high-quality films, and sputtering process parameters that can greatly impact the properties of the films. Therefore, the purpose of this paper is to undertake the overview of the sputtering of high entropy alloys with the emphasis on the sputtering process parameter influences on the quality of HEA, mechanisms of formation, and the deposition process. The paper will serve as a significant resource for the HEA optimization studies for industrial applications.

3. Sputtering process parameter-property relationship of high entropy alloys

There are numerous factors that can influence the sputtering of high entropy alloys such as the deposition parameters, substrate temperature, and the post-processing treatment (Mwema et al., 2019; Oladijo et al., 2021; Surmenev et al., 2017;

Simon, 2018), and a summary of the factors that are influencing the sputtered HEA deposition is presented in Table 1. From the Table, power, temperature, substrate bias and pressure are significant process parameters on deposition of HEAs thin films.

Power: sputtering power plays a role in both the films deposition and the film thickness formation during the sputtering (deposition) process (Ejaz et al., 2022). Atoms sputter more often as a result of high-energy Ar ions attacking the target when the sputtering power is increased (Surmenev et al., 2017). With increased power, the deposition rate likewise rises, which causes the film thickness to increase. It is clear from studies done on the film deposition of (AlCrMnMoNiZr)_N HEA film published by Ren et al. shows that increasing power in the region of 150 W - 350 W led to increases in the deposition rate (Ren et al., 2014).

Temperature: The systems sputtering temperature also has an impact on the film thickness and improve the film quality (Zhang et al., 2013). Adatom diffusion rate and mobility rise with substrate temperature, causing the production of larger grains, a smoother surface, a decrease in surface roughness, an increase in the film's resistance to corrosion, and also controlling the adherence of the film (Dai et al., 2020; Parau et al., 2022; Sun et al., 2020; Vladescu et al., 2015). Therefore, to achieve a higher temperature, the substrate material is often positioned on a heating stage. However, when sputtering takes place, the sputtering itself generates heat as a result of atoms colliding on the surface (Ejaz et al., 2022). Hence, the film deposited might be harmed by excessive heating (Ejaz et al., 2022). As a result, cooling is necessary in cases of excessive heat, and a study is needed to determine the material's maximum required temperature.

Substrate Bias: The optical and microstructural properties of thin films sputtered would be altered by substrate bias (Zhang et al., 2019). It slows down the rate at which films are deposited but the size of the grains increases (Zhang et al., 2019). Substrate bias during deposition increases the kinetic energies of the particles on the coating; as a result, the mobility of the atoms producing the film increases, leading to tinner coatings, larger crystalline grain coatings and greater metallic state transfer (Zhang et al., 2019). The impact of film characteristics on substrate bias was studied by Xu Yu et al (Yu et al., 2021). by sputtering CrNbSiTiZr HEAs films at various substrate bias voltages. The outcome shows that the film densification and the re-sputtering effect are to blame for the deposition rate decrease with increasing substrate bias. Also, as the bias increases, the atomic mobility to the surface increases, causing the columnar structure to change into a dense structure.

Sputtering pressure: At high sputtering pressures, bombarded particles are thermalized before they reach the film's surface; therefore, there mechanism (atomic peening) is weakened (Iriarte et al., 2011). Compressive stress is usually related to a mechanism (atomic peening) in which rebounding neutral atoms impact the forming film at minimal sputtering pressures (Iriarte et al., 2011). The frequency of gaseous phase collisions rises with increasing sputtering pressure, which lowers the sputtered kinetic energy neutral atoms and reflects neutrals bombarding the expanding film (Iriarte et al., 2011). This decrease in the atomic peening decreases compressive stress. Additionally, the average distance (mean free path (λ)) between particles sputtered before with gas atoms depends on the gas working pressure. While, as the sputtering pressure drops, the (kinetic) energy mobility from the plasma to the forming film surface is increased. The working pressure has an inverse relationship with the λ . The λ will be closer as the gas pressure rises, and the ejected atoms will collide more before depositing on the substrate, which may lead to a low deposition rate and reduction in film thickness. Therefore, the sputtering is mostly conducted at low pressures of below 5 m toor to avoid the sputtered atoms being subjected to too many gas phase collisions, and evacuate the vacuum to $<10^{-5}$ Toor, in order to prevent contamination and maintain clean surfaces from leftover (residual) gas molecules, forming on the surface of the substrate (Ghazal & Sohail, 2023).

Table 1. Sputtering process parameter-property relationship for HEAs thin films

Target; Substrate	Deposition method	Aim of the research	The deposition parameters	Findings	Ref
AlCrSiTiMoO; Si	DC-magnetron sputtering	To investigate the working pressure effect on the hardness, morphology, chemical composition, growth mechanism, and topography of the surface of the film.	Sputtering time of 30min; the power of 200 W; distance between substrate and target is 80 mm; etching voltage of 500 V; base pressure at Torr of 9×10^{-5} ; and pressure at 1, 4, 8, and 12 mTorr. The sputtered specimen was denoted as S1, S4, S8 & S12 relating to the working pressure varied.	<ul style="list-style-type: none"> ✓ The result obtained revealed that the hardness of the film deposited decreases as the sputtering pressure increases. The finding was attributed to argon gas that is backscattered when impinging on the surface of the substrate. ✓ The result of the morphology reveals that the Si surface is very smooth with no void or defect, while the morphology changes as the pressure is increased especially for S4 & S8 which roughness increased to 2 nm. ✓ The deposited layer's chemical composition changes with the changes in the pressure such as the oxygen content decreasing at S8 while other element % increase. ✓ 	(Behravan et al., 2021)

Target; Substrate	Deposition method	Aim of the research	The deposition parameters	Findings	Ref
FeCoNiAlMnW; Si	RF magnetron sputtering	To investigate the effect of substrate temperature on the microstructure, mechanical properties, and film growth.	Sputtering power of 90 W; the substrate rotation speed of 2 r/min; base pressure of 4.0×10^{-4} Pa, argon gas of 0.4 Pa, substrate deposition of 20°C, 200°C, 400°C, and 600°C;	<ul style="list-style-type: none"> ✓ The XRD result obtained revealed that all the samples sputtered at different temperatures are crystalline, and the films were all BCC-structure solid solutions. ✓ The thin film surface becomes smoother as the temperature of the substrate increases to 600°C. ✓ . ✓ Increase in the substrate temperature led to the bigger grains, higher roughness, less defect & larger internal stress. 	(Sun et al., 2020)
AlCoCrCu _{0.5} FeNi. Si (100) wafers and quartz	RF reactive magnetron sputtering	To investigate the influence of RF power process parameter on the HEA films microstructure, and physical properties	Base pressure of 7.5×10^{-7} ; substrate holder rotating speed of 20rpm; substrate to target distance of 150mm, working pressure of 10mTorr; temp of 250°C; RF power of 200W, 250W & 300W; and the sputtered time was adjusted to have similar films thickness.	<ul style="list-style-type: none"> ✓ The result obtained from the coating shows the HEA film thickness increases as the rf power increases. ✓ The XRD result showed that the film is polycrystalline with the mixture of phases of BCC & FCC ✓ The crystallinity of the film increases as the power increases. ✓ The XPS revealed presence of Cr₂O₃ & Al₂O₃ protective oxide film on all the coated samples. ✓ The HEA hydrophobicity films improved with an increase in the rf power, and the film sputtered at maximum power showed the maximum hydrophobicity with 129° contact angle 	(Khan et al., 2020)
Al _x CoCrFeNi; Si	magnetron sputtering	To investigate the Al _x CoCrFeNi HEAs films resistivity temperature behaviors	Working distance of 100mm; substrate rotation of 10rpm; base pressure of 4×10^{-4} Pa; argon flowrate of 10sccm; working pressure of 1.40Pa; dc power of 100W at 60min sputtering time; rf power of 100W at 30min and 90min;	<ul style="list-style-type: none"> ✓ The result obtained revealed that all the films exhibit consistent characteristics, smooth film-substrate interface, and uniform thickness. ✓ The result of the films obtained shows that the films have good crystallization and are composed of BCC and FCC phases columnar grains. ✓ The films exhibit an ultra-low temperature coefficient resistance within the ± 10ppm/K range, and their resistivity is beyond conventional alloy film reach. 	(C. Wang et al., 2020)
AlCrMnMoNiZr; Si	RF magnetron sputtering	To investigate the sputtering temperature and power on HEAs films.	Nitrogen flow ratio (RN) of 0.5 N ₂ /Ar; rf power of 350W for substrate temperature of 300K, 500K, and 600K; substrate temperature of 500K for rf power of 150W, 250W, and 350W; coating distance of 75mm; substrate rotation of 60rpm; sputtering time of 2 hr.	<ul style="list-style-type: none"> ✓ The result revealed the element content and the deposition rate increased with an increase in the sputtering power. ✓ The film crystallization increased with an increase in the sputtering temperature and power. ✓ The film at high deposition power exhibited a smooth surface and the increased in the substrate temperature led to coarse grains and higher surface roughness and high hardness. ✓ Low coefficient of friction and high hardness are obtained at 250W power and 600 K temperature. 	(Ren et al., 2014)
NbTiAlSiZrN _x ; Quartz glass	Magnetron sputtering	To investigate the sputtered (NbTiAlSiZr) _{N_x} HEC films thermal stability and mechanical properties at high temperature	Working pressure of 0.6Pa; the power of 100W; argon flowrate of 24sccm; nitrogen flow rate of 0,4, and 8sccm; sputtering time of 40min;	<ul style="list-style-type: none"> ✓ The result obtained from the XRD revealed the films exhibit complete amorphous phase structure, and after annealing the films exhibit an amorphous broad peak phase. ✓ Nano crystallization occurred in the coating at nitrogen flowrate of 4 and 8sccm after annealing for 900°C at 30min, and the film exhibit an FCC structure. ✓ The film exhibits high hardness at RT. 	(Xing et al., 2018)

Target; Substrate	Deposition method	Aim of the research	The deposition parameters	Findings	Ref
AlTiCrNiT; Zr-4	RF magnetron sputtering	The investigation of high temperature and mechanical properties of AlTiCrNiTa HEA film deposited by rf magnetron sputtering for the fuel cladding accident tolerant	Power of 150W; tempt of 200°C; Ar argon of 0.4 Pa; substrate rotation of 5rpm; substrate to target distance of 5cm	<ul style="list-style-type: none"> ✓ The microstructure result obtained from the SEM revealed that film-coated is dense, uniform, and near-equal molar continuous ratio. ✓ The coating is amorphous and FCC structure. ✓ The coating has a high hardness of 18.34 and high corrosion resistance. 	(S. Zhao et al., 2021)
AlCoCrNi; Si	Reactive DC magnetron sputtering	To investigate the AlCoCrNi thin film mechanical and microstructural properties and the optimization of the sputtering parameters	Process pressure of 1.33×10^{-1} , 3.33×10^{-1} , 6.67×10^{-1} , and 1.33 Pa; base pressure of $< 3.33 \times 10^{-4}$ Pa; nitrogen flow rate of 25,50,75, and 100 % RN; power of 300W; rotation speed of 10rpm; temperature at RT; gas flow of 20sccm.	<ul style="list-style-type: none"> ✓ The result obtained revealed that an increase in the RN during the sputtering led to decreasing in the AlCoCrNi nitride deposition rate. ✓ The result obtained showed the AlCoCrNi HEN films are amorphous phase with near equiatomic composition ratios, regardless of the ratio of the Nitrogen flow conditions and the process pressure. ✓ The result obtained revealed that increased in the process pressure led to increase in the collision between the deposited process gas and atoms in the chamber, which led to decrease in the mean free path, and result to low adatoms mobility which as a result, led to less dense microstructure (open structure and porous). ✓ The hardness, elasticity modulus and H/E ratios of the film increased with decreasing in the process pressure. 	(Kim, Park, Lim, et al., 2019)
TiTaHfNbZr. Ti-6Al-4V	RF magnetron sputtering	To investigate the tribological behavior and microstructure of the equimolar TiTaHfNbZr high entropy alloy sputtered on Ti-6Al-4V for biomedical application.	Base pressure of 1×10^{-5} Pa; the temperature at RT; Ar of 10 (SCCM); the power of 100W;	<ul style="list-style-type: none"> ✓ The HEA film displays an amorphous phase with fine-grained homogeneous surface topography. ✓ The HEA film increases the Ti-6Al-4V elastic modulus and hardness and as a result improved the material tribological properties, such as the coefficient of friction and wear resistance. 	(Tüten et al., 2019a)
CoCrFeMnNi; silicon	RF magnetron sputtering	To investigate the mechanical properties effect of CoCrFeNiMn HEA coating	The substrate to target distance of 8cm; substrate holder rotating speed of 2rpm; argon flow of 22 sccm; temp at RT; sputtering time of 30 min; rf power of 350 W.	<ul style="list-style-type: none"> ✓ The SEM result showed the film has a homogenous and smooth surface without any defect and a thickness of ~300 nm. ✓ The microstructural result obtained from the TEM and XRD reveal the film is composed of both phase of BCC and FCC solid solution. ✓ The result showed increased in the hardness and ductility of the HEA film which is higher than the bulk material. 	(Dang et al., 2018)
AlFeCrNiMo; SS 304	magnetron sputtering	To study the AlFeCrNiMo HEA coatings and stainless steel 304 tribological effect	The sputtering current of 0.8 A; sputtering time of 180min. and after sputtering, treated, and cooled in vacuum at 30 min and 300°C.	<ul style="list-style-type: none"> ✓ The result obtained from the SEM image revealed the surface of the substrate is uniformly distributed with almost no pores or crack on the surface. ✓ The hardness result revealed that the HEA coating hardness increases and higher than the hardness of the stainless steel 304. ✓ The result obtained revealed that the sputtered HEA coating wear resistance increases comparing to the 304 SS bulk material under same tribo corrosion condition. ✓ The result obtained revealed the HEA coating has lower corrosion current and higher corrosion potential which shows that the coating has better resistance to corrosion in artificial seawater. 	(Zeng & Xu, 2020)

Target; Substrate	Deposition method	Aim of the research	The deposition parameters	Findings	Ref
CuMoTaWV; Si and SS 304	DC magnetron sputtering	To study the influence of refractory high entropy alloys (RHEA) CuMoTaWV film via magnetron sputtering mechanical characterization and synthesis.	Substrate holder rotation speed of 8rpm; the power of 150W; sputtering time of 120min; deposition pressure of 1.16×10^{-3} mPa; substrate temperature of 500°C; the gas flow of 20scm. And after, annealed in an argon atmosphere at 300°C with the rate of the heat of 2°C / min.	<ul style="list-style-type: none"> ✓ The result obtained from the SEM analysis revealed that the RHEA film morphology is needle-like, and the cross-section revealed a dense and morphology textured with uniform thickness. ✓ The Cu addition to the RHEA coatings led to an increase in the nanopillar compressional strength and the hardness. ✓ The result obtained revealed the adhesion, wear resistance and coefficient of friction of the coating improved by the annealing of the coating. 	(Alvi et al., 2020a)
(CrTaTiVZr)N; Si	RF magnetron sputtering	To investigate the sputtered (CrTaTiVZr)N film characteristics and structure	Working pressure of 6.67×10^{-1} ; rf power of 350W; Ar flowrate of 100scm; N2 flowrate of 4scm; substrate bias of 0-200V; substrate to target distance of 90mm; substrate temperature of 450°C; sputtering time of 60min.	<ul style="list-style-type: none"> ✓ The result obtained revealed that target element concentration is almost not affected by the varied substrate bias and the nitrogen content decreases slightly with increases in the substrate bias. ✓ The XRD result revealed increases in the substrate bias led to XRD diffraction peaks shift and broadening and slightly decreasing in the grain size. ✓ Increased in the substrate bias result to the coating microstructure changes from the structure that is typical columnar to fine fiber and dense structure. 	(Chang et al., 2015)
TiZrHfNiCuCo; tungsten carbide (WC)	DC magnetron sputtering	To investigate the mechanical and structural properties of TiZrHfNiCuCo thin film that is synthesized via magnetron sputtering	The temperature at RT; substrate holder of 10 rpm; Argon flow of 20 scm; the power of 100 W to 300 W; sputtering time of 30 to 90 min at 300W.	<ul style="list-style-type: none"> ✓ The result obtained revealed that the thickness of the film increases as the sputtering power and the deposition time increase. ✓ The result obtained from the TEM and the XRD revealed that the HEA films are an amorphous phase, while the N2 reactive gas addition led to a rise in the single-phase FCC type nano crystallite formation of the HEA nitride coatings. ✓ The result obtained from the nanoindentation revealed that the TiZrHfNiCuCo nitride coating has greater elastic modulus and hardness than TiZrHfNiCuCo metallic coatings. 	(Kim, Park, Mun, et al., 2019)
(AlCrMnMoNiZr B _{0.1})Nx; Si	DC magnetron sputtering	The investigation of microstructure, chemical composition, tribological and mechanical properties of (AlCrMnMoNiZrB _{0.1}) Nx film	Working distance of 75mm; working pressure of 2 Pa; target power of 80W; base pressure of 8.0×10^{-3} Pa; substrate bias of 0V; rotation of the substrate at 40rpm; substrate temperature of 500K; sputtering time of 120min and nitrogen flow ratio (RN) of 0, 0.2, 0.5, 0.8 and 1.0	<ul style="list-style-type: none"> ✓ The HEA films at 0 and 0.2 RN display an amorphous structure; in contrast, FCC solid solution structure was seen on the other nitride films. ✓ The XRD result showed the film structure changes from the amorphous phase to mixed and finally to crystalline phase structure with increase in the nitrogen content. ✓ The RN increases with decreases in the cluster size and at 1.0 RN the film columnar crystal changes to dense structure with a smooth surface, and the surface roughness decreases. ✓ Increases in the RN led to increases in the hardness, coefficient of friction, metallic film modulus and resistance to wear increases. 	(Ren et al., 2011)
AlCoCrCu0.5FeNi ; quartz and Si wafer	reactive magnetron sputtering	To investigate the nanostructured AlCoCrCu0.5FeNi HEA film deposited by reactive magnetron sputtering.	substrate holder rotation at 20rpm; temp at 250°C; the power of 30-0W; working pressure of 10mTorr; gas flow of 15scm and the sputtering was varied to get a thickness of approximately 100nm	<ul style="list-style-type: none"> ✓ The result obtained revealed that an increase in the oxygen flowrate led to the decrease in the rate of deposition and decrease in the average grain size. ✓ The film with RN of 12.5 % exhibit dome shape topography and the highest surface roughness, while the surface roughness reduces with the increased in the oxygen flow rate and the topography of the surfacer change to a needler like structure. 	(Khan et al., 2021)

Target; Substrate	Deposition method	Aim of the research	The deposition parameters	Findings	Ref
				<ul style="list-style-type: none"> ✓ The result obtained from the nanoindentation showed the intermediate coating of 25% has the highest hardness. ✓ The coating at 50% has the highest water contact angle of 111° 	
AlCoFeNiTiZr; Si	RF magnetron sputtering	The investigation of the corrosion behavior and microstructure of the AlCoFeNiTiZr HEA film coating	The gas flow rate of 80sccm; the temperature of 100°C; working pressure of 0.1Pa; three x.% of 15, 20, and 25, with power (Fe-Ce-Ni target) of 250, 270, 300W, Power /w (Al-Ti-Zr target) of 35, 33, 30 and the sputtering time of 90, 90 and 100min respectively.	<ul style="list-style-type: none"> ✓ The result obtained showed the film form nanocrystalline and large amorphous phases. ✓ The result obtained revealed an increase in the content of Fe-Co-Ni result to the growth and aggregation of the crystal which led to the decrease in the intercrystalline corrosion. ✓ The coating showed an excellent anti-corrosion property, and the film Ecorr increase positively, while Icorr value decreases with increases in the content, with film with x=25 displaying the maximum level of corrosion resistance. 	(Wang et al., 2020b)
NbTiAlSiZrNx; Stainless steel 304	Rf magnetron sputtering	To study the sputtered NbTiAlSiZrNx films corrosion resistance and mechanical properties	Pressure of 0.6Pa; Ar gas flow rate of 25sccm; voltage of 600V; current of 180mA; rf power of 120W; pulse frequency of 13.56MHz; nitrogen flowrate of 0,3,6,11,17 and 25sccm; deposition time of 60min. working distance of 60mm and vacuum pressure of 6x10 ⁻⁴ Pa.	<ul style="list-style-type: none"> ✓ The result obtained revealed the film thickness decreases as the RN increases from 20%-50%. ✓ The film surface roughness increases with an increase in the RN from 10% to 50 %, and the surface roughness at 30% was the highest of all. ✓ The modulus and surface hardness increased with an increase in the RN. ✓ The XRD result shows the samples diffraction phase all had an amorphous structure. ✓ The resistance to corrosion of the film was high, and the coating at 30% N2 flowrate had the lowest corrosion resistance. 	(Xing et al., 2019)

4. Properties of sputtered High Entropy Alloy thin films

Despite the fact that sputtered HEA films have only been investigated for a few decades, extraordinary physical, chemical, and mechanical properties, such as excellent elastic modulus and hardness, superior corrosion and wear resistance, temperature resistance, in addition to appealing magnetic and electrical properties, have already been achieved.

4.1 Mechanical properties

HEAs film coating produced using the sputtering deposition process have a considerable impact on the mechanical properties of the bulk (substrate) material (Zhao et al., 2013; Lv et al., 2016). (Tan et al., 2021) investigates the mechanical properties of HEA film by sputtering CoCrFeNi on silicon (P-type single-crystal). The result obtained revealed the films are FCC phase and coating surface are dense and smooth. While the increase in the substrate bias led to an increase in the hardness, elastic modulus, and creep properties of the film. Chang et al (Chang et al., 2019) investigated the HEA nitride film's mechanical properties by sputtering (AlCrNbSiTiV)N on glass and cutting tool inserts (cermet T1200A, and TNMG160404R-UM) via dc magnetron sputtering. The result obtained reveals that the film's adhesion strength is good, and the hardness of the films reached a 2493HV value, 6.96 mN nanoindentation peak force loading, and 47.92% elastic recovery. Figures 3 show the summary of the comparison of hardness properties results of various sputtered HEAs thin films coatings from the literature (Garah et al., 2022; Liang et al., 2020; Yang et al., 2021; Huang et al., 2022; Khan et al., 2021; Kretschmer et al., 2021; Muftah et al., 2021a; Sha et al., 2020a; Xing et al., 2019; Xu et al., 2021; Medina et al., 2021), and Figure 4 shows the summary of the comparison of different elastic modulus of sputtered HEAs thin films coatings from the literature (Alvi et al., 2020b; Cai et al., 2021; Feng et al., 2013; Zhao et al., 2013; Kim, Park, Lim, et al., 2019; Chen et al., 2020; Lv et al., 2016; Ren et al., 2011; Tan et al., 2021; W. Liao et al., 2017b). Furthermore, existing research on HEAs demonstrates that nitride films made of the entire nitride element created higher hardness than those made of non-nitride producing elements (such as Co, Cu, Fe, Ni, and Mn) (Chen et al., 2020). Moreover, HEAs films with basic cubic structures have a low hardness, which when nitrogen atoms are added, creates strong Me-N bonds in the film and deepens the degrees of lattice distortion. When the amount of nitrogen is increased until it reaches its maximum saturation, the impact of strengthening the solid solution is enhanced, and the film elastic modulus and hardness both rise. Hence, in Fig. 3 and Fig. 4, AlCrTiZrV, which is made up of all-nitride metal components and has the addition of V to cause it to react with nitrogen to generate vanadium nitride, with a hexagonal and FCC structure, produced the highest levels of hardness and elastic modulus, while HEAs made up of non-nitride elements produced lower levels of hardness and elastic modulus.

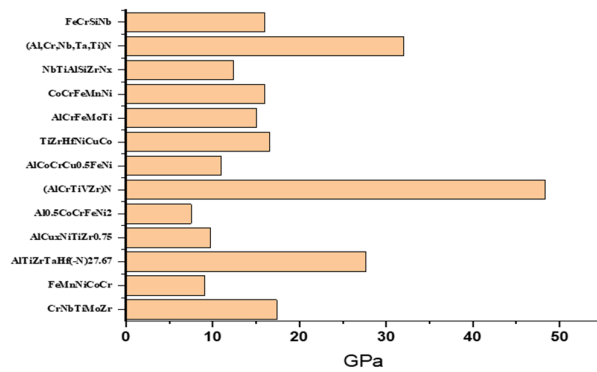


Fig. 3. Comparison of hardness properties of various sputtered HEA thin film coatings.

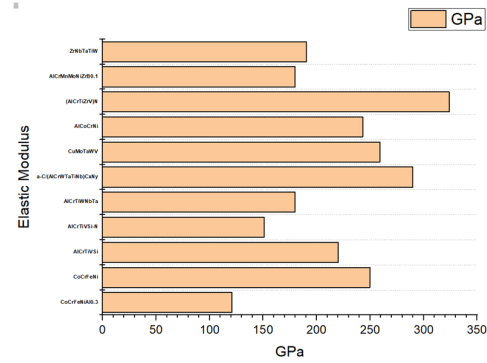


Fig. 4. Comparison of different sputtered HEA thin film elastic modulus.

4.2 Corrosion properties

High entropy alloys films have a diverse set of applications due to their excellent corrosion resistance behaviour (Muftah et al., 2021b). Wang et al. (Wang et al., 2020b) investigate the corrosion behaviours and microstructure of HEAs film by sputtering AlCoFeNiTiZr on Si. The result obtained reveals that The HEAs film exhibited good anticorrosion capabilities, indicating that it has the potential to be used in corrosive situations. Chen et al. (Chen et al., 2005) investigate the HEA film electrochemical and microstructure properties with the comparison with stainless steel 304. The result reveals that HEA has less resistant to pitting corrosion in chloride conditions than SS 304, which accounts for the lesser pitting potential and a smaller range of potentials in the passive zone. Furthermore, Bachani, et al. (Bachani et al., 2020) investigates the corrosion behaviours, mechanical and microstructural properties of HEA coating, and the effect of the content of Aluminium. VNbMoTaW and VNbMoTaWAl refractory HEA were sputtered on stainless steel 304 and Si substrates. The result obtained reveals the substrate corrosion resistance increase by the HEA film and the best corrosion was obtained by the AL addition. Table 2 shows the result of different HEA coatings electrochemical corrosion test.

The Ni, Cr, Ti, Mo, and Co elements are recognized to be positive to boost the corrosion resistance in acid solutions in the HEAs multi-principal element compositions. While, contrarily, it has been claimed that the elements Cu, Mn, and Al have a negative influence on anti-corrosion (Li et al., 2019); Although the additional component elements could have different outcomes. Thus, it is crucial to carry out actual experimental research on the electrochemical behaviors of various HEA-based coatings under various processing conditions. Furthermore, By addition of carbon (Ca), Medina et al. (Medina et al., 2021) examine the CoCrFeMnNi coatings. The findings show that film corrosion resistance increased with increasing Ca concentration and is marginally greater than for hyper-duplex SS made for extremely corrosive circumstances. The film showed (Fe-Co-Ni) 25(Al-Ti-Zr)75 HEAs. Wang et al. (Wang et al., 2020a) examine the AlCoFeNiTiZr HEA's corrosion behaviour. The result revealed that the (Fe-Co-Ni)₂₅(Al-Ti-Zr)₇₅ HEAs film demonstrated good corrosion resistance and offered a promising material for use in highly corrosive situations. Additionally, the results demonstrate that the active metals Fe, Zr, and Al created multiple microelectrodes and changed into a cation surrounded by an anion. While the matching Al, Ti, and Zr oxides created the passivation layers to stop further corrosion. Furthermore, Due to the exceptional design flexibility of HEAs in physical metallurgy, HEA characteristics can be modified to satisfy various needs, such as corrosion resistance, by adding passivating metals like Cr, Ti, Ni, Mo, and Al to each sample. The combination of a number of characteristics, most of which are connected to chemical homogeneity with regard to elemental distribution via grain boundaries and crystalline phases, determines the corrosion resistance of multi-principal element alloys. Passive film stability is crucial in this context and careful composition management is, therefore, necessary to provide the highest performance against corrosion. The alloying materials and development of a homogenous microstructure affect the passive film's stability.

Table 2. Different types of HEA coatings corrosion result

HEA	I _{corr} (A/cm ²)	E _{corr} , v	Reference
FeCrSiNb	8.56*E-12	0.27	(Muftah et al., 2021b)
FeCrMnNiC	2.5*E-10	0.07	(Muftah et al., 2020)
CrMnFeCoNi	1.1*E-7	-0.09	(Mehmood et al., 2022)
CoCuFeMnNiTi0.1	1.89 *E -5	-0.401	(Öztürk et al., 2022)
CoCuFeMnNi	6.30 *E -7	-0.322	(Öztürk et al., 2022)
CoCuFeMnNiTi0.4	1.03 *E -3	-0.961	(Öztürk et al., 2022)
AlTiCrNiTa	3.2*E-8	-0.26	(Wang et al., 2020a)
CoCrFeNiW	1.4*E-5	-0.99	(Shang et al., 2017)

4.3 Biocompatibility properties

High entropy alloys film has excellent biocompatibility properties. Peighambardoust et al. (Peighambardoust et al., 2021) investigate refractory HEA film in vitro biocompatibility for orthopedic implants application. By sputtering Ti_{1.5}ZrTa_{0.5}Nb_{0.5}Hf_{0.5} RHEA film on with a SS316L, Ti6Al4V and CoCrMo. The result obtained reveals that the film can be regarded as a prospective and protective coating on biomaterials because it is composed of non-toxic and allergy-free refractory elements. Also, the EIS measurement reveals that the sputtered sample's charge transfer resistance is notably high, at about $1.5 \times 10^7 \Omega \text{ cm}^2$, as a result of the substrate and target excellent adhesion. Furthermore, Chen et al. (Chen et al., 2020), investigate the HEA film's biocompatibility and bio-corrosion by coating Ti-33Ta-33Nb MEA and Ti-10Ta-6Nb films on Si ater (p-type (100) via co-sputtering pure Nb, Ti, and Ta targets. The result obtained reveals that HEA film significantly increased hardness, wear resistance, biocompatibility, and bio-corrosion resistance. In vitro biocompatibility and bio-corrosion behavior of equimolar TiZrHfNbTa HEA were studied by Yang et al. (Yang et al., 2020), The film demonstrated good bio-corrosion resistance in 310K Hank's solution, has good viability and adhesion, and also the proliferation of MC3T3-E1 pre-osteoblasts on film suggested that they were well-biocompatible in vitro. Additionally, the XPS study of the alloy surface revealed that the excellent HEA bio-corrosion resistance is due to the creation of a passive coating made up of ZrO₂, TiO₂, HfO₂, Ta₂O₅, and Nb₂O₅. Furthermore, Cemin et al. (Cemin et al., 2022), study the excellent in vitro biocompatibility in sputtered NbTaTiVZr(O) HEA metallic glass coatings. The results of the in vitro biocompatibility tests employing the MG-63 osteosarcoma cells and hTERT-immortalized bone marrow mesenchymal both demonstrated great vitality (96% and 98%, respectively) and good adherence on to HEMG films after 96 h of incubation, suggesting the biosafety and integrity of this surface. which demonstrates that it has potential for use as a bio coating for orthopaedic implants and sputtering (Cemin et al., 2022) is efficient for depositing biomaterial due to is good cell adhesion and healthy cell morphologies.

4.4 Tribological properties

The HEA films acquire high hardness, as was already indicated, which would enable them to significantly lower the rate of wear. The mechanical properties of the coatings often dictate their tribological characteristics. Because of this, it is anticipated that HEA films coatings will exhibit exceptional wear resistance, which has been confirmed by several studies on their tribological behaviors (Kao et al., 2021a; Sha et al., 2020b). Tüten et al. (2019b) investigates the sputtered TiTaHfNbZr HEA on Ti-6Al-4V microstructure and tribological behavior. The result obtained reveals HEA provides much-improved surface protection against cracking and wear, which could be particularly useful in long-term orthopedic implants that are subjected to dynamic contact stress, such as hip or knee joints. Cai et al. investigate the tribological behaviors of HEA film. By sputtering AlCrTiVSi and AlCrTiV on stainless steel. The result obtained reveals that the HEA film greatly improved the tribological properties of the material (Cai et al., 2021). Kao et al. (Kao et al., 2021b), investigate the sputtered High-entropy TaNbSiZrCr coatings on WC substrates. The results show that the coatings have excellent tribological characteristics, including good wear resistance $0.33 \text{ E}^{-6} \text{ mm}^3/\text{Nm}$ and a stable, low CoF of 0.09. Table 3, show the structural, hardness and tribological properties of sputtered HEA film.

Table 3. Different types of sputtered HEA coatings microstructure, hardness, friction coefficient and wear rate.

Target	Method used	phases	Hardness	Friction coefficient	Wear rate ($\times 10^{-5} \text{ mm}^3 \text{ N}^{-1} \text{ m}^{-1}$)	Design approach	Ref; year
CrNbTiMoZr	DC magnetron sputtering	Amorphous + BCC		0.5	x	Process enhancement	(Wang et al., 2020)
TiZrNbTaFe	high power impulse magnetron sputtering (HiPIMS)	Amorphous	36.2 GPa	0.69	0.075	Process enhancement	(Wang et al., 2020)
(AlCrWTiMo)N	DC magnetron sputtering	FCC		0.65	1.1	Process enhancement	(Wang et al., 2022)
VAlTiCrMo	magnetron sputtering	BCC	10.35 GPa	0.53	11.6	Compositional design	(Fan et al., 2022)
TaNbSiZrCr	RF unbalanced magnetron sputtering	FCC and Amorphous	34.1 GPa	0.09	0.033	Compositional design	(Kao et al., 2021b)
CrAlNbSiV/N	RF magnetron sputtering	FCC	28-35 GPa	0.88	0.2	Process enhancement	(Lin et al., 2020)
AlTiTaZrHf(-N)	reactive magnetron sputtering	FCC and amorphous	27.67 GPa	0.7	x	Process enhancement	(Garah et al., 2022)
AlCrTiVSi.N	DC magnetron sputtering	BCC	16.55 GPa	0.55	2.12	Compositional design	(Cai et al., 2021)
(AlCrMoTaTiZr)Nx	RF reactive magnetron sputtering	FCC	40 GPa	0.74	0.28	Process enhancement	(Cheng et al., 2011)
CrTaNbMoV	DC magnetron sputtering	BCC	21.6 GPa	0.50	5.2	Compositional design	(Feng et al., 2020)
CrNbSiTiZr/Cx	RF magnetron sputtering	FCC	32 GPa	0.07	0.02	Compositional design	(Jhong et al., 2018)

4.5 Structural properties

Amorphous, BCC or FCC solid-solution phase are frequently forms in HEA films coatings. This is as a result of the restraining impacts on the nucleation and elements diffusion of the intermetallic phases, which is a result of the preparation processes used to produce HEA films and coatings. Al_{0.3}CoCrFeNi HEAs Films Produced by Magnetron Sputtering was studied by Liao et al (Liao et al., 2019). The outcome demonstrates a uniform chemical composition with a single FCC structure for the HEA thin film. A single BCC phase mainly composed each of the VAlTiCrCu HEA films, regardless of the deposition temperature (Chen et al., 2019). Dolique et al. (2009) investigated the association between complex composition and sputtered AlCoCrCuFeNi HEA. They discovered that three distinct structures were formed, including amorphous, FCC, and BCC solid-solution phases, indicating that even a little change in the chemical structure might cause a structure transition. Sputtered nano crystalline Al_x (CoCrFeNi)_{100-x} combinatorial HEAs coating shows the crystal structures of thin films change from FCC to BCC as the quantity of Al increases. The BCC and FCC films both exhibit a consistent elemental distribution (Shi et al., 2020b). The (FeCoCrNi)_{1-x}(WC)_x HEAs microstructures composites are made up of four phases: M₂₃C₆-type carbide, WC-type carbide, M₇C₃-type carbides, and FCC matrix phase (Zhou et al., 2018). According to the findings of the investigation on the structure properties of a-C/(AlCrWTaTiNb)_{C_xN_y} composite films. the result shows an AlCrWTaTiNb multi-element nitride film made without the Ca target exhibits a triangle-shaped morphology with 2-phase FCC. And when the Ca target power is between 50 and 150 W, the composites film crystallographic structure converts to single-phase FCC and to granular morphology (Lv et al., 2016). In a study of sputtered CoCrFeNi HEAs films, the result shows it composed of FCC phase, and the elements were distributed evenly on a dense and smooth surface (Tan et al., 2021). In a research by Garah et al. (Garah et al., 2022), high entropy metal-sub lattice nitrides of AlTiTaZrHf(-N) were sputtered and then deposited on silicon and glass substrates in varied argon–nitrogen gas compositions. The outcome shows that the film transitioned from an amorphous phase to an FCC single phase by raising the N content. Based on the N flow rate, the shape of the films can be either columnar or compact. Additionally, EDS analysis reveals a decrease in the metal content when the ratio of the N flow rates $R_{N2} = N_2/Ar+N_2$, rises.

Based on a review of the above-discussed properties of sputtered HEA films, it can be observed that sputtering is a significant method for depositing HEA films. Also, HEA has improved hardness, with AlCrTiZrV/N HEA film having superior hardness and modulus when compared to other HEA films from Figures 3 and 4. Furthermore, as a result of its exceptional qualities, such as higher hardness and strength, which are exactly what wear-resistant materials require, high entropy alloy (HEA) also exhibits excellent corrosion and wear resistance. The solid strengthening effect of solid solution and the second phase strengthening resulting from hard compounds in HEA efficiently improve the capability of the coating to resist deformation, it benefits from having a diversity of primary elements, which leads to higher entropy, and the phase structure, such as a large number of amorphous or nanocrystals in the alloy, optimizes the material properties of the material.

4.6 Sputtered HEA Applications

High entropy alloys are a type of sophisticated material that has exceptional properties. It can be sputtered on bulk materials to take benefit of both thin-film and substrate materials due to the cost of production. Thin films have become a vital part of industrial and scientific operations because of their significant effect. By increasing the surface properties quality of the materials and making the material more versatile and suitable for a variety of applications. The following generic areas can be used to organize the HEA thin-film applications.

4.7 Biomedical applications

Due to HEAs outstanding mechanical qualities and biocompatibility, HEAs are a subclass of biomaterials which biomedical applications have recently undergone intensive exploration (Patil et al., 2022). Sputtered High Entropy Alloys are a potential material that can be used for medical applications due to their exceptional film qualities such as superior wear and corrosion resistance, biocompatibility, osseointegration, and remarkable polarization resistance (Öztürk et al., 2022; Patil et al., 2022; Shi et al., 2020a; Zhou et al., 2018). And, also the adhesion properties from the sputtering deposition techniques, owing to the strong bonding between the film and the substrate material (Aksoy et al., 2019; Chu et al., 2014; Gökmenoğlu et al., 2016; Peighambardoust et al., 2021; Braic et al., 2012). Metallic biomaterials like Co-Cr-Mo, 316L, and Ti-6Al-4V exhibit poor corrosion and wear resistance along with limited biocompatibility. In order to solve this problem, the idea of RHEAs was developed. TiZrTaHfNb and Ta-Zr-Hf-Nb display exceptional wear and corrosion resistance, wettability, low young modulus, non-toxic, and allergy-free (Patil et al., 2022). According to Tüten et al. (Tüten et al., 2019b), analysis of the sputtered Ti-Ta-Hf-Nb-Zr HEA films, the result reveals the film markedly enhanced the biocompatibility, wear and corrosion behaviors of the material, and would be useful, particularly for long-term implant applications that support dynamic contact stress, like knee or hip joints. Using co-sputtering, Braic et al. (Braic et al., 2012), study the characteristics of multi-principal element (TiZrNbHfTa)C and (TiZrNbHfTa)N HEA film for biomedical devices. The findings show that the coatings have excellent corrosion-wear resistance, low friction coefficient, high hardness, and outstanding biocompatible properties. And, would be highly helpful in long-term orthopedics that undergo contact angle loadings, such as knee or hips. Additionally, orthopaedic devices implant such as knee joints, hip joints, scaffolds, bone screws, spinal fusion cages, ligament and shoulder joints, and bone plates can primarily be made using HEAs biomedical material.

4.8 Structural and Industrial application

Sputtered HEAs have the potential for structural and industrial applications. In the aerospace sector, materials utilized as modern engine components must endure high translation speeds, fatigue cracks, creep, and harsh operating temperatures (Dada et al., 2021; Khan et al., 2019b). Therefore, the components made must be compact and have strong strength at elevated temperatures, be fatigue-resistant, immune to chemical deterioration, corrosion and wear resistance, and be resistant to oxidation (Dada et al., 2021). HEAs offer excellent properties such as outstanding work hardenability, good ductility, and high-temperature oxidation resistance (Zhang et al., 2014). They have very effective magnetic properties and good wear-corrosion resistance (Zhang et al., 2014). This property makes HEAs exceptional refractory materials for variety of structural aircraft engine applications. Additionally, their outstanding qualities enable the fabrication of components like the turbine component engine (combustor, compressor, turbine blade and nozzle) (Dada et al., 2021). Alvi et al. (Alvi et al., 2020a) investigate the HEA synthesis and mechanical characterization effects by sputtering CuMoTaWV. The result obtained reveals HEA is beneficial for nanopillar, wear, and large-scale industrial applications. Khan et al. (Khan et al., 2019a) investigate the impact of sputtered AlCoCrCu_{0.5}FeNi HEA film. The result revealed that sputtered HEAs films have the potential to be used as a protective and hard covering for energy and aerospace applications. AlCoCrCu_{0.5}FeNi (Khan et al., 2019b), AlTiZrTaHf(-N) (Garah et al., 2022), CoCrFeNiAl (Liao et al., 2017a) and other HEAs series have the potential to be used in structural and industrial applications.

4.9 Energy electrocatalysis application

Due to sputtered HEA's outstanding properties, next-generation energy technologies have piqued researchers' interests. However, to overcome the sluggish cardiac reaction kinetics, these technologies require efficient and robust electrocatalysts. Due to their rich structural motifs and morphological features, sputtered HEA nanostructures films created by easy, adaptable, and green sputtering processes have exceptional electrochemical performances, demonstrating tremendous promise for enhancing reaction kinetics and as a result, there's a potential to speed up the development of the next energy technologies (Liang et al., 2021). According to Chen et al. (Chen et al., 2022) study of the convex cube-shaped PtFeNiCuMoRu HEAs catalyst for strong multipurpose electrocatalysis. the result reveals the HEA catalysts exhibit outstanding electrocatalytic performance for the hydrogen evolution, oxygen evolution, and oxygen reduction reaction, MnFeCoNiCu, IrOsPdPtRhRu, CoFeLaNiP, AlNiCoIrMo, PdFeCoNiCu, AuAgPtPdCu series (Zhang et al., 2022), and so on are HEAs catalyst that can be used for energy electrocatalysis application due to their outstanding stabilities and activity in electrochemical reactions related to storage and energy conversion

5. Future Scope

Over the last two decades, a lot of effort has gone into researching sputtered HEA films. Various HEA thin films have already demonstrated attractive features such as high elastic modulus and hardness, exceptional wear, temperature, and corrosion resistance, as well as appealing magnetic and electrical behaviours properties. The HEA's future work is proposed in this section.

1. High entropy alloys' corrosion resistance can be effectively increased by properly combining elements like Co, Al, Ti, Mo, and Cr, whereas HEAs that include the full nitride element have greater mechanical qualities. In order to further understand how different crystalline phases affect HEAs' ability to resist corrosion, scanning strong probe techniques like (scanning electrochemical microscopy) should be employed with proper combination of HEAs element, while based on design requirements like mechanical properties, the mixing of intermetallic compounds and solid solutions, the residual stresses, and the addition of numerous lubricious materials, research into the introduction of additional elements (such as nitrogen) during sputtering to improve HEA qualities should be explored, developed, considered, and put into practice.
2. There is a paucity of simulation and modelling literature on sputtered HEA thin films, which is a useful tool for elucidating linkages between preparation procedures, and properties. More research on predictive computer modelling of sputtered HEA thin films is needed.

6. Conclusions

Trends and advances made in the field of sputtered HEA thin film was discussed in this article, which reveals that sputtered HEA film have demonstrated attractive and exceptional properties as a branch of HEA material for over two decades. The HEA thin films, sputtering processes, review of sputtered HEAs properties of sputtered HEA films, and sputtered HEAs applications were also presented and discussed. The various reasons and design factors for the excellent properties are examined, as well as proposed research avenues for future sputtering of HEA films. This paper reveals sputtered HEA thin films have excellent mechanical properties, including high elastic modulus, hardness, and wear resistance. Additionally, the biocompatible, physical, and oxidation resistances of the sputtered HEA thin films were discussed, as well as their unique corrosion resistance, high phase stability, and desirable magnetic, electrical, and biocompatible properties. These findings

indicate that the sputtered HEA thin films can have mechanical properties at high temperatures, excellent oxidation resistance, and high phase stability. There are also numerous sputtering process parameters that relate to the causes of the excellent qualities and the design elements that led to them.

Acknowledgement

The authors would like to acknowledge the University Research Committee (URC) of the University of Johannesburg for bursary offered to the first co-author.

References

- Abegunde, O., Akinlabi, E. T., & Oladijo, P. (2019). Substrate effect on the morphology, structural and tribology properties of Titanium carbide thin film grown by RF Magnetron Sputtering. *Journal of Physics: Conference Series*, 1378(2).
- Aksoy, C. B., Canadinc, D., & Yagci, M. B. (2019). Assessment of Ni ion release from TiTaHfNbZr high entropy alloy coated NiTi shape memory substrates in artificial saliva and gastric fluid. *Materials Chemistry and Physics*, 236(June), 121802.
- Aliyu, A., & Srivastava, C. (2019). Microstructure and corrosion properties of MnCrFeCoNi high entropy alloy-graphene oxide composite coatings. *Materialia*, 5(November 2018), 100249.
- Alvi, S., Jarzabek, D. M., Kohan, M. G., Hedman, D., Jenczyk, P., Natile, M. M., Vomiero, A., & Akhtar, F. (2020a). Synthesis and Mechanical Characterization of a CuMoTaWV High-Entropy Film by Magnetron Sputtering. *ACS Applied Materials and Interfaces*, 12(18), 21070–21079.
- Alvi, S., Jarzabek, D. M., Kohan, M. G., Hedman, D., Jenczyk, P., Natile, M. M., Vomiero, A., & Akhtar, F. (2020b). Synthesis and Mechanical Characterization of a CuMoTaWV High-Entropy Film by Magnetron Sputtering. *ACS Applied Materials & Interfaces*, 12(18), 21070–21079.
- Arif, Z. U., Khalid, M. Y., Al Rashid, A., ur Rehman, E., & Atif, M. (2022). Laser deposition of high-entropy alloys: A comprehensive review. *Optics & Laser Technology*, 145(August 2021), 107447.
- Ayyagari, A., Barthelemy, C., Gwalani, B., Banerjee, R., Scharf, T. W., & Mukherjee, S. (2018). Reciprocating sliding wear behavior of high entropy alloys in dry and marine environments. *Materials Chemistry and Physics*, 210, 162–169.
- Ayyagari, A. V., Gwalani, B., Muskeri, S., Mukherjee, S., & Banerjee, R. (2018). Surface degradation mechanisms in precipitation-hardened high-entropy alloys. *Npj Materials Degradation*, September.
- Bachani, S. K., Wang, C.-J., Lou, B.-S., Chang, L.-C., & Lee, J.-W. (2020). Microstructural characterization, mechanical property and corrosion behavior of VNbMoTaWAl refractory high entropy alloy coatings: Effect of Al content. *Surface and Coatings Technology*, 403(August), 126351.
- Behravan, N., Farhadizadeh, A., Ghasemi, S., Khademi, A., Shojaei, H., & Ghomi, H. (2021). The pressure dependence of structure and composition of sputtered AlCrSiTiMoO high entropy thin film. *Journal of Alloys and Compounds*, 852, 156421.
- Braeckman, B. R., Boydens, F., Hidalgo, H., Dutheil, P., Jullien, M., Thomann, A.-L., & Depla, D. (2015a). High entropy alloy thin films deposited by magnetron sputtering of powder targets. *Thin Solid Films*, 580, 71–76.
- Braeckman, B. R., Boydens, F., Hidalgo, H., Dutheil, P., Jullien, M., Thomann, A. L., & Depla, D. (2015b). High entropy alloy thin films deposited by magnetron sputtering of powder targets. *Thin Solid Films*, 580, 71–76.
- Braic, M., Balaceanu, M., Vladescu, A., Zoita, C. N., & Braic, V. (2013). Deposition and characterization of multi-principal-element (CuSiTiYzr)C coatings. *Applied Surface Science*, 284, 671–678.
- Braic, V., Balaceanu, M., Braic, M., Vladescu, A., Panseri, S., & Russo, A. (2012). Characterization of multi-principal-element (TiZrNbHfTa)N and (TiZrNbHfTa)C coatings for biomedical applications. *Journal of the Mechanical Behavior of Biomedical Materials*, 10, 197–205.
- Cai, Z., Wang, Z., Hong, Y., Lu, B., Liu, J., Li, Y., & Pu, J. (2021). Improved tribological behavior of plasma-nitrided AlCrTiV and AlCrTiVSi high-entropy alloy films. *Tribology International*, 163(June), 107195.
- Cantor, B., Chang, I. T. H., Knight, P., & Vincent, A. J. B. (2004). Microstructural development in equiatomic multicomponent alloys. *Materials Science and Engineering: A*, 375–377(1-2 SPEC. ISS.), 213–218.
- Cemin, F., Luis Artico, L., Piroli, V., Andrés Yunes, J., Alejandro Figueroa, C., & Alvarez, F. (2022). Superior in vitro biocompatibility in NbTaTiVZr(O) high-entropy metallic glass coatings for biomedical applications. *Applied Surface Science*, 596(May).
- Chang, C. H., Li, P. W., Wu, Q. Q., Wang, M. H., Sung, C. C., & Hsu, C.-Y. (2019). Nanostructured and mechanical properties of high-entropy alloy nitride films prepared by magnetron sputtering at different substrate temperatures. *Materials Technology*, 34(6), 343–349. <https://doi.org/10.1080/10667857.2018.1557411>
- Chang, Z.-C., Tsai, D.-C., & Chen, E.-C. (2015). Structure and characteristics of reactive magnetron sputtered (CrTaTiVZr)N coatings. *Materials Science in Semiconductor Processing*, 39, 30–39.
- Chen, L., Li, W., Liu, P., Zhang, K., Ma, F., Chen, X., Zhou, H., & Liu, X. (2020). Microstructure and mechanical properties of (AlCrTiZrV)Nx high-entropy alloy nitride films by reactive magnetron sputtering. *Vacuum*, 181(August), 109706.
- Chen, S., Cai, Z., Lu, Z., Pu, J., Chen, R., Zheng, S., Mao, C., & Chen, S. (2019). Tribo-corrosion behavior of VAlTiCrCu high-entropy alloy film. *Materials Characterization*, 157(August), 109887.
- Chen, T., Wu, W., Li, W., & Liu, D. (2019). Laser cladding of nanoparticle TiC ceramic powder: Effects of process parameters on the quality characteristics of the coatings and its prediction model. *Optics & Laser Technology*, 116(March), 345–355.

- Chen, Y. H., Chuang, W. S., Huang, J. C., Wang, X., Chou, H. S., Lai, Y. J., & Lin, P. H. (2020). On the bio-corrosion and biocompatibility of TiTaNb medium entropy alloy films. *Applied Surface Science*, *508*, 145307.
- Chen, Y. Y., Duval, T., Hung, U. D., Yeh, J. W., & Shih, H. C. (2005). Microstructure and electrochemical properties of high entropy alloys—a comparison with type-304 stainless steel. *Corrosion Science*, *47*(9), 2257–2279.
- Chen, Z., Wen, J., Wang, C., & Kang, X. (2022). Convex Cube-Shaped Pt₃₄Fe₅Ni₂₀Cu₃₁Mo₉Ru High Entropy Alloy Catalysts toward High-Performance Multifunctional Electrocatalysis. *Small*, *18*(45), 1–9. <https://doi.org/10.1002/sml.202204255>
- Cheng, K.-H., Lai, C.-H., Lin, S.-J., & Yeh, J.-W. (2011). Structural and mechanical properties of multi-element (AlCrMoTaTiZr)_{Nx} coatings by reactive magnetron sputtering. *Thin Solid Films*, *519*(10), 3185–3190.
- Chu, J. P., Liu, T. Y., Li, C. L., Wang, C. H., Jang, J. S. C., Chen, M. J., Chang, S. H., & Huang, W. C. (2014). Fabrication and characterizations of thin film metallic glasses: Antibacterial property and durability study for medical application. *Thin Solid Films*, *561*, 102–107.
- Dada, M., Popoola, P., Adeosun, S., & Mathe, N. (2021). High Entropy Alloys for Aerospace Applications. In *Aerodynamics*. IntechOpen.
- Dai, C., Fu, Y., Guo, J., & Du, C. (2020). Effects of substrate temperature and deposition time on the morphology and corrosion resistance of FeCoCrNiMo_{0.3} high-entropy alloy coating fabricated by magnetron sputtering. *International Journal of Minerals, Metallurgy and Materials*, *27*(10), 1388–1397.
- Dang, C., Surjadi, J. U., Gao, L., & Lu, Y. (2018). Mechanical properties of nanostructured CoCrFeNiMn high-entropy alloy (HEA) coating. *Frontiers in Materials*, *5*(August), 1–6.
- Deng, L., Bai, C., Jiang, Z., Luo, J., Tu, J., Xu, H., Huang, H., Tan, L., & Ding, L. (2021). Effect of B₄C particles addition on microstructure and mechanical properties of Fe₅₀Mn₃₀Co₁₀Cr₁₀ high-entropy alloy. *Materials Science and Engineering: A*, *822*(June), 141642.
- Depla, D. (2021). Sputter deposition with powder targets: An overview. *Vacuum*, *184*(September), 109892.
- Diao, H. Y., Feng, R., Dahmen, K. A., & Liaw, P. K. (2017). Fundamental deformation behavior in high-entropy alloys : An overview. *Current Opinion in Solid State & Materials Science*, *21*(5), 252–266.
- Dolique, V., Thomann, A.-L., Brault, P., Tessier, Y., & Gillon, P. (2009). Complex structure/composition relationship in thin films of AlCoCrCuFeNi high entropy alloy. *Materials Chemistry and Physics*, *117*(1), 142–147.
- Ejaz, H., Hussain, S., Zahra, M., Saharan, Q. M., & Ashiq, S. (2022). Several sputtering parameters affecting thin film deposition. *Journal of Applied Chemical Science International*, *April*, 41–49.
- El Garah, M., Touaibia, D. E., Achache, S., Michau, A., Sviridova, E., Postnikov, P. S., Chehimi, M. M., Schuster, F., & Sanchette, F. (2022). Effect of nitrogen content on structural and mechanical properties of AlTiZrTaHf(-N) high entropy films deposited by reactive magnetron sputtering. *Surface and Coatings Technology*, *432*(December 2021), 128051.
- Fan, J., Liu, X., Pu, J., & Shi, Y. (2022). Anti-friction mechanism of VAlTiCrMo high-entropy alloy coatings through tribo-oxidation inducing layered oxidic surface. *Tribology International*, *171*(December 2021), 107523.
- Feng, X., Tang, G., Sun, M., Ma, X., Wang, L., & Yukimura, K. (2013). Structure and properties of multi-targets magnetron sputtered ZrNbTaTiW multi-elements alloy thin films. *Surface and Coatings Technology*, *228*(SUPPL.1), S424–S427.
- Feng, X., Zhang, K., Zheng, Y., Zhou, H., & Wan, Z. (2020). Chemical state, structure and mechanical properties of multi-element (CrTaNbMoV)_{Nx} films by reactive magnetron sputtering. *Materials Chemistry and Physics*, *239*(July 2019), 121991.
- George, E. P., Raabe, D., & Ritchie, R. O. (2019). High-entropy alloys. *Nature Reviews Materials*, *4*(8), 515–534.
- Ghazal, H., & Sohail, N. (2023). Sputtering Deposition. In *Thin Films - Deposition Methods and Applications* (Vol. 25, Issue 4, pp. e275–e281). IntechOpen. <https://doi.org/10.5772/intechopen.107353>
- Gökmenoğlu, C., Özmeric, N., Cakal, G., Dökmetaş, N., Ergene, C., & Kaftanoğlu, B. (2016). Coating of titanium implants with boron nitride by RF-magnetron sputtering. *Bulletin of Materials Science*, *39*(5), 1363–1370.
- Huang, K., Wang, G., Qing, H., Chen, Y., & Guo, H. (2022). Effect of Cu content on electrical resistivity, mechanical properties and corrosion resistance of AlCu NiTiZr_{0.75} high entropy alloy films. *Vacuum*, *195*(August), 110695.
- Iriarte, G. F., Rodriguez, J. G., & Calle, F. (2011). Effect of substrate–target distance and sputtering pressure in the synthesis of AlN thin films. *Microsystem Technologies*, *17*(3), 381–386.
- Jhong, Y. S., Huang, C. W., & Lin, S. J. (2018). Effects of CH₄ flow ratio on the structure and properties of reactively sputtered (CrNbSiTiZr)_{Cx} coatings. *Materials Chemistry and Physics*, *210*, 348–352.
- Kao, W. H., Su, Y. L., Horng, J. H., & Wu, H. M. (2021a). Effects of carbon doping on mechanical, tribological, structural, anti-corrosion and anti-glass-sticking properties of CrNbSiTaZr high entropy alloy coatings. *Thin Solid Films*, *717*(July 2020), 138448.
- Kao, W. H., Su, Y. L., Horng, J. H., & Wu, W. C. (2021b). Mechanical, tribological, anti-corrosion and anti-glass sticking properties of high-entropy TaNbSiZrCr carbide coatings prepared using radio-frequency magnetron sputtering. *Materials Chemistry and Physics*, *268*(May), 124741.
- Kawagishi, K., Sato, A., Harada, H., Yeh, A.-C., Koizumi, Y., & Kobayashi, T. (2009). Oxidation resistant Ru containing Ni base single crystal superalloys. *Materials Science and Technology*, *25*(2), 271–275.
- Kemény, D. M., Miskolcziné Pálfi, N., & Fazakas, É. (2021). Examination of microstructure and corrosion properties of novel AlCoCrFeNi multicomponent alloy. *Materials Today: Proceedings*, *45*, 4250–4253.
- Khan, N. A., Akhavan, B., Zheng, Z., Liu, H., Zhou, C., Zhou, H., Chang, L., Wang, Y., Liu, Y., Sun, L., Bilek, M. M., & Liu, Z. (2021). Nanostructured AlCoCrCu_{0.5}FeNi high entropy oxide (HEO) thin films fabricated using reactive

- magnetron sputtering. *Applied Surface Science*, 553(August 2020), 149491.
- Khan, N. A., Akhavan, B., Zhou, C., Zhou, H., Chang, L., Wang, Y., Liu, Y., Fu, L., Bilek, M. M., & Liu, Z. (2020). RF magnetron sputtered AlCoCrCu_{0.5}FeNi high entropy alloy (HEA) thin films with tuned microstructure and chemical composition. *Journal of Alloys and Compounds*, 836, 155348.
- Khan, N. A., Akhavan, B., Zhou, H., Chang, L., Wang, Y., Sun, L., Bilek, M. M., & Liu, Z. (2019a). High entropy alloy thin films of AlCoCrCu_{0.5}FeNi with controlled microstructure. *Applied Surface Science*, 495(July).
- Khan, N. A., Akhavan, B., Zhou, H., Chang, L., Wang, Y., Sun, L., Bilek, M. M., & Liu, Z. (2019b). High entropy alloy thin films of AlCoCrCu_{0.5}FeNi with controlled microstructure. *Applied Surface Science*, 495(July), 143560.
- Kim, Y. S., Park, H. J., Lim, K. S., Hong, S. H., & Kim, K. B. (2019). Structural and Mechanical Properties of AlCoCrNi High Entropy Nitride Films: Influence of Process Pressure. *Coatings*, 10(1), 10. <https://doi.org/10.3390/coatings10010010>
- Kim, Y. S., Park, H. J., Mun, S. C., Jumaev, E., Hong, S. H., Song, G., Kim, J. T., Park, Y. K., Kim, K. S., Jeong, S. Il, Kwon, Y. H., & Kim, K. B. (2019). Investigation of structure and mechanical properties of TiZrHfNiCuCo high entropy alloy thin films synthesized by magnetron sputtering. *Journal of Alloys and Compounds*, 797, 834–841. <https://doi.org/10.1016/j.jallcom.2019.05.043>
- Kishore Reddy, C., Gopi Krishna, M., & Srikant, P. (2019). Brief Evolution Story and some Basic Limitations of High Entropy Alloys (HEAs) – A Review. *Materials Today: Proceedings*, 18, 436–439.
- Kretschmer, A., Kirnbauer, A., Moraes, V., Primetzhofer, D., Yalamanchili, K., Rudigier, H., & Mayrhofer, P. H. (2021). Improving phase stability, hardness, and oxidation resistance of reactively magnetron sputtered (Al,Cr,Nb,Ta,Ti)N thin films by Si-alloying. *Surface and Coatings Technology*, 416(April), 127162.
- Lei, Z., Liu, X., Wu, Y., Wang, H., Jiang, S., Wang, S., Hui, X., Wu, Y., Gault, B., Kontis, P., Raabe, D., Gu, L., Zhang, Q., Chen, H., Wang, H., Liu, J., An, K., Zeng, Q., Nieh, T., & Lu, Z. (2018). *Enhanced strength and ductility in a high-entropy alloy via ordered oxygen complexes*.
- Li, J., Huang, Y., Meng, X., & Xie, Y. (2019). A Review on High Entropy Alloys Coatings: Fabrication Processes and Property Assessment. *Advanced Engineering Materials*, 21(8), 1900343.
- Li, W., Liu, P., & Liaw, P. K. (2018). Microstructures and properties of high-entropy alloy films and coatings: a review. *Materials Research Letters*, 6(4), 199–229.
- Liang, J.-T., Cheng, K.-C., Chen, Y.-C., Chiu, S.-M., Chiu, C., Lee, J.-W., & Chen, S.-H. (2020). Comparisons of plasma-sprayed and sputtering Al_{0.5}CoCrFeNi₂ high-entropy alloy coatings. *Surface and Coatings Technology*, 403(September), 126411.
- Liang, J., Liu, Q., Li, T., Luo, Y., Lu, S., Shi, X., Zhang, F., Asiri, A. M., & Sun, X. (2021). Magnetron sputtering enabled sustainable synthesis of nanomaterials for energy electrocatalysis. *Green Chemistry*, 23(8), 2834–2867.
- Liao, W.-B., Zhang, H., Liu, Z.-Y., Li, P.-F., Huang, J.-J., Yu, C.-Y., & Lu, Y. (2019). High Strength and Deformation Mechanisms of Al_{0.3}CoCrFeNi High-Entropy Alloy Thin Films Fabricated by Magnetron Sputtering. *Entropy*, 21(2), 146.
- Liao, W., Lan, S., Gao, L., Zhang, H., Xu, S., Song, J., Wang, X., & Lu, Y. (2017a). Nanocrystalline high-entropy alloy (CoCrFeNiAl_{0.3}) thin-film coating by magnetron sputtering. *Thin Solid Films*, 638, 383–388.
- Liao, W., Lan, S., Gao, L., Zhang, H., Xu, S., Song, J., Wang, X., & Lu, Y. (2017b). Nanocrystalline high-entropy alloy (CoCrFeNiAl_{0.3}) thin-film coating by magnetron sputtering. *Thin Solid Films*, 638, 383–388.
- Lin, S.-Y., Chang, S.-Y., Huang, Y.-C., Shieu, F.-S., & Yeh, J.-W. (2012). Mechanical performance and nanoindenting deformation of (AlCrTaTiZr)NCy multi-component coatings co-sputtered with bias. *Surface and Coatings Technology*, 206(24), 5096–5102.
- Lin, Y. C., Hsu, S. Y., Song, R. W., Lo, W. L., Lai, Y. T., Tsai, S. Y., & Duh, J. G. (2020). Improving the hardness of high entropy nitride (Cr_{0.35}Al_{0.25}Nb_{0.12}Si_{0.08}V_{0.20})N coatings via tuning substrate temperature and bias for anti-wear applications. *Surface and Coatings Technology*, 403(101), 126417.
- Lv, C. F., Zhang, G. F., Cao, B. S., He, Y. Y., Hou, X. D., & Song, Z. X. (2016). Structure and mechanical properties of a-C/(AlCrWTaTiNb)C_xN_y composite films. *Surface Engineering*, 32(7), 541–546.
- Market, T., & Electronics, M. (2010). Deposition Technologies: An Overview. In *Handbook of Deposition Technologies for Films and Coatings* (Third Edit, pp. 1–31). Elsevier. <https://doi.org/10.1016/B978-0-8155-2031-3.00001-6>
- Mehmood, K., Umer, M. A., Munawar, A. U., Imran, M., Shahid, M., Ilyas, M., Firdous, R., Kousar, H., & Usman, M. (2022). Microstructure and Corrosion Behavior of Atmospheric Plasma Sprayed NiCoCrAlFe High Entropy Alloy Coating. *Materials*, 15(4), 1486.
- Miracle, D. B. (2019). High entropy alloys as a bold step forward in alloy development. *Nature Communications*, 1–3. <https://doi.org/10.1038/s41467-019-09700-1>
- Muftah, W., Allport, J., & Vishnyakov, V. (2021a). Corrosion performance and mechanical properties of FeCrSiNb amorphous equiatomic HEA thin film. *Surface and Coatings Technology*, 422(May), 127486.
- Muftah, W., Allport, J., & Vishnyakov, V. (2021b). Corrosion performance and mechanical properties of FeCrSiNb amorphous equiatomic HEA thin film. *Surface and Coatings Technology*, 422(June), 127486.
- Muftah, W., Patmore, N., & Vishnyakov, V. (2020). Demanding applications in harsh environment – FeCrMnNiC amorphous equiatomic alloy thin film. *Materials Science and Technology*, 36(12), 1301–1307.
- Mwema, F. M., Akinlabi, E. T., Oladijo, O. P., & Baruwa, A. D. (2020). Advances in Powder-based Technologies for Production of High-Performance Sputtering Targets. *Materials Performance and Characterization*, 9(4), 20190160.
- Mwema, F. M., Akinlabi, E. T., Oladijo, O. P., & Majumdar, J. D. (2019). Effect of varying low substrate temperature on

- sputtered aluminium films. *Materials Research Express*, 6(5), 056404.
- Oladijo, S., Akinlabi, E., Mwema, F., & Stamboulis, A. (2021). An Overview of Sputtering Hydroxyapatite for Biomedical Application. *IOP Conference Series: Materials Science and Engineering*, 1107(1), 012068.
- Oluwatosin Abegunde, O., Titilayo Akinlabi, E., Philip Oladijo, O., Akinlabi, S., & Uchenna Ude, A. (2019). Overview of thin film deposition techniques. *AIMS Materials Science*, 6(2), 174–199.
- Oses, C., Toher, C., & Curtarolo, S. (2020). High-entropy ceramics. *Nature Reviews Materials*, 5(4), 295–309.
- Öztürk, S., Alptekin, F., Önal, S., Sünbül, S. E., Şahin, Ö., & İcin, K. (2022). Effect of titanium addition on the corrosion behavior of CoCuFeNiMn high entropy alloy. *Journal of Alloys and Compounds*, 903, 163867.
- Parau, A. C., Cotrut, C. M., Guglielmi, P., Cusanno, A., Palumbo, G., Dinu, M., Serratore, G., Ambrogio, G., Vranceanu, D. M., & Vladescu, A. (2022). Deposition temperature effect on sputtered hydroxyapatite coatings prepared on AZ31B alloy substrate. *Ceramics International*, 48(8), 10486–10497.
- Patil, V., Balivada, S., & Appagana, S. (2022). Biomedical Applications of Titanium and Aluminium-based High Entropy Alloys. *International Journal of Health Technology*, 1(1), 40–48.
- Peighambaroust, N. S., Alamdari, A. A., Unal, U., & Motallebzadeh, A. (2021). In vitro biocompatibility evaluation of Ti1.5ZrTa0.5Nb0.5Hf0.5 refractory high-entropy alloy film for orthopedic implants: Microstructural, mechanical properties and corrosion behavior. *Journal of Alloys and Compounds*, 883, 160786.
- Praveen, S., & Kim, H. S. (2018). High-Entropy Alloys: Potential Candidates for High-Temperature Applications – An Overview. *Advanced Engineering Materials*, 20(1), 1–22. <https://doi.org/10.1002/adem.201700645>
- Qiu, Y., Thomas, S., Gibson, M. A., Fraser, H. L., & Birbilis, N. (2017). Corrosion of high entropy alloys. *Npj Materials Degradation*, January, 1–17.
- Ren, B., Liu, Z. X., Shi, L., Cai, B., & Wang, M. X. (2011). Structure and properties of (AlCrMnMoNiZrB0.1)N_x coatings prepared by reactive DC sputtering. *Applied Surface Science*, 257(16), 7172–7178.
- Ren, B., Lv, S.-J., Zhao, R.-F., Liu, Z.-X., & Guan, S.-K. (2014). Effect of sputtering parameters on (AlCrMnMoNiZr)N films. *Surface Engineering*, 30(2), 152–158.
- Samaei, A., Mirsayar, M., & Aliha, M. (2015). The microstructure and mechanical behavior of modern high temperature alloys. *Engineering Solid Mechanics*, 3(1), 1–20.
- Schwarz, H., Uhlig, T., Rösch, N., Lindner, T., Ganss, F., Hellwig, O., Lampke, T., Wagner, G., & Seyller, T. (2021). CoCrFeNi High-Entropy Alloy Thin Films Synthesised by Magnetron Sputter Deposition from Spark Plasma Sintered Targets. *Coatings*, 11(4), 468.
- Senkov, O. N., Wilks, G. B., Miracle, D. B., Chuang, C. P., & Liaw, P. K. (2010). Refractory high-entropy alloys. *Intermetallics*, 18(9), 1758–1765.
- Sha, C., Zhou, Z., Xie, Z., & Munroe, P. (2020a). High entropy alloy FeMnNiCoCr coatings: Enhanced hardness and damage-tolerance through a dual-phase structure and nanotwins. *Surface and Coatings Technology*, 385(February), 125435.
- Sha, C., Zhou, Z., Xie, Z., & Munroe, P. (2020b). High entropy alloy FeMnNiCoCr coatings: Enhanced hardness and damage-tolerance through a dual-phase structure and nanotwins. *Surface and Coatings Technology*, 385(December 2020), 125435.
- Shang, C., Axinte, E., Sun, J., Li, X., Li, P., Du, J., Qiao, P., & Wang, Y. (2017). CoCrFeNi(W1-xMox) high-entropy alloy coatings with excellent mechanical properties and corrosion resistance prepared by mechanical alloying and hot pressing sintering. *Materials & Design*, 117, 193–202.
- Sharma, A. (2021). High Entropy Alloy Coatings and Technology. *Coatings*, 11(4), 372. <https://doi.org/10.3390/coatings11040372>
- Shi, Y., Yang, B., Rack, P. D., Guo, S., Liaw, P. K., & Zhao, Y. (2020a). High-throughput synthesis and corrosion behavior of sputter-deposited nanocrystalline Al_x(CoCrFeNi)_{100-x} combinatorial high-entropy alloys. *Materials and Design*, 195, 109018.
- Shi, Y., Yang, B., Rack, P. D., Guo, S., Liaw, P. K., & Zhao, Y. (2020b). High-throughput synthesis and corrosion behavior of sputter-deposited nanocrystalline Al (CoCrFeNi)₁₀₀- combinatorial high-entropy alloys. *Materials & Design*, 195, 109018.
- Simon, A. H. (2018). Sputter Processing. In *Handbook of Thin Film Deposition* (Second Edi, pp. 195–230). Elsevier.
- Sun, X., Cheng, X., Cai, H., Ma, S., Xu, Z., & Ali, T. (2020). Microstructure, mechanical and physical properties of FeCoNiAlMnW high-entropy films deposited by magnetron sputtering. *Applied Surface Science*, 507(November 2019), 145131.
- Surmenev, R. A., Surmeneva, M. A., Grubova, I. Y., Chernozem, R. V., Krause, B., Baumbach, T., Loza, K., & Epple, M. (2017). RF magnetron sputtering of a hydroxyapatite target: A comparison study on polytetrafluorethylene and titanium substrates. *Applied Surface Science*, 414, 335–344.
- Surmenev, R., Vladescu, A., Surmeneva, M., Ivanova, A., Braic, M., Grubova, I., & Cotrut, C. M. (2017). Radio Frequency Magnetron Sputter Deposition as a Tool for Surface Modification of Medical Implants. In *Modern Technologies for Creating the Thin-film Systems and Coatings* (pp. 214–248). InTech.
- Tan, S., Liu, X., & Wang, Z. (2021). Nanoindentation mechanical properties of CoCrFeNi high entropy alloy films. *Materials Technology*, 00(00), 1–12.
- Tüten, N., Canadinc, D., Motallebzadeh, A., & Bal, B. (2019a). Intermetallics Microstructure and tribological properties of TiTaHfNbZr high entropy alloy coatings deposited on Ti e 6Al e 4V substrates. *Intermetallics*, 105(November 2018), 99–106.
- Tüten, N., Canadinc, D., Motallebzadeh, A., & Bal, B. (2019b). Microstructure and tribological properties of TiTaHfNbZr

- high entropy alloy coatings deposited on Ti 6Al 4V substrates. *Intermetallics*, 105(August 2018), 99–106.
- Vladescu, A., Braic, M., Azem, F. A., Titorencu, I., Braic, V., Pruna, V., Kiss, A., Parau, A. C., & Birlık, I. (2015). Effect of the deposition temperature on corrosion resistance and biocompatibility of the hydroxyapatite coatings. *Applied Surface Science*, 354, 373–379.
- Wang, C., Li, X., Li, Z., Wang, Q., Zheng, Y., Ma, Y., Bi, L., Zhang, Y., Yuan, X., Zhang, X., Dong, C., & Liaw, P. K. (2020). The resistivity–temperature behavior of Al CoCrFeNi high-entropy alloy films. *Thin Solid Films*, 700(September 2019), 137895.
- Wang, H., Liu, J., Xing, Z., Ma, G.-Z., Cui, X., Jin, G., & Xu, B. (2020a). Microstructure and corrosion behaviour of AlCoFeNiTiZr high-entropy alloy films. *Surface Engineering*, 36(1), 78–85.
- Wang, H., Liu, J., Xing, Z., Ma, G., Cui, X., Jin, G., & Xu, B. (2020b). *Microstructure and corrosion behaviour of AlCoFeNiTiZr high-entropy alloy films*. 0844.
- Wang, J., Kuang, S., Yu, X., Wang, L., & Huang, W. (2020). Tribo-mechanical properties of CrNbTiMoZr high-entropy alloy film synthesized by direct current magnetron sputtering. *Surface and Coatings Technology*, 403(August), 126374.
- Wang, Y., He, N., Wang, C., Li, J., Guo, W., Sui, Y., & Lan, J. (2022). Microstructure and tribological performance of (AlCrWTiMo)N film controlled by substrate temperature. *Applied Surface Science*, 574(August 2021), 151677.
- Wu, W., Jiang, L., Jiang, H., Pan, X., Cao, Z., Deng, D., Wang, T., & Li, T. (2015). Phase Evolution and Properties of Al₂CrFeNiMo_x High-Entropy Alloys Coatings by Laser Cladding. *Journal of Thermal Spray Technology*, 24(7), 1333–1340.
- Xing, Q., Wang, H., Chen, M., Chen, Z., Li, R., Jin, P., & Zhang, Y. (2019). Mechanical Properties and Corrosion Resistance of NbTiAlSiZrN_x High-Entropy Films Prepared by RF Magnetron Sputtering. *Entropy*, 21(4), 396. <https://doi.org/10.3390/e21040396>
- Xing, Q., Xia, S., & Yan, X. (2018). *Mechanical properties and thermal stability of (NbTiAlSiZr) N_x high-entropy ceramic films at high temperatures*. 3347–3354.
- Xu, Y., Li, G., Li, G., Gao, F., & Xia, Y. (2021). Effect of bias voltage on the growth of super-hard (AlCrTiVZr)N high-entropy alloy nitride films synthesized by high power impulse magnetron sputtering. *Applied Surface Science*, 564(March), 1–10.
- Yalamanchili, K., Wang, F., Schramm, I. C., Andersson, J. M., Johansson Jöesaar, M. P., Tasnádi, F., Mücklich, F., Ghafoor, N., & Odén, M. (2017). Exploring the high entropy alloy concept in (AlTiVNbCr)N. *Thin Solid Films*, 636, 346–352.
- Yang, J., Shi, K., Chen, Q., Zhang, W., Zhu, C., Ning, Z., Liao, J., Yang, Y., Liu, N., & Yang, J. (2021). Effect of Au-ion irradiation on the surface morphology, microstructure and mechanical properties of amorphous AlCrFeMoTi HEA coating. *Surface and Coatings Technology*, 418(March), 127252.
- Yang, W., Liu, Y., Pang, S., Liaw, P. K., & Zhang, T. (2020). Bio-corrosion behavior and in vitro biocompatibility of equimolar TiZrHfNbTa high-entropy alloy. *Intermetallics*, 124(March), 106845.
- Yeh, J. W., Chen, S. K., Lin, S. J., Gan, J. Y., Chin, T. S., Shun, T. T., Tsau, C. H., & Chang, S. Y. (2004). Nanostructured high-entropy alloys with multiple principal elements: Novel alloy design concepts and outcomes. *Advanced Engineering Materials*, 6(5), 299–303.
- Yoosefan, F., Ashrafi, A., Mahmoud, S., & Constantin, I. (2020). Synthesis of CoCrFeMnNi High Entropy Alloy Thin Films by Pulse Electrodeposition : Part 1 : Effect of Pulse Electrodeposition Parameters. *Metals and Materials International*, 26(8), 1262–1269.
- Yu, X., Wang, J., Wang, L., & Huang, W. (2021). Fabrication and characterization of CrNbSiTiZr high-entropy alloy films by radio-frequency magnetron sputtering via tuning substrate bias. *Surface and Coatings Technology*, 412(December 2020), 127074.
- Zendejas Medina, L., Riekehr, L., & Jansson, U. (2020). Phase formation in magnetron sputtered CrMnFeCoNi high entropy alloy. *Surface and Coatings Technology*, 403(April), 126323.
- Zendejas Medina, L., Tavares da Costa, M. V., Paschalidou, E. M., Lindwall, G., Riekehr, L., Korvela, M., Fritze, S., Kolozsvári, S., Gamstedt, E. K., Nyholm, L., & Jansson, U. (2021). Enhancing corrosion resistance, hardness, and crack resistance in magnetron sputtered high entropy CoCrFeMnNi coatings by adding carbon. *Materials and Design*, 205.
- Zeng, Q., & Xu, Y. (2020). A comparative study on the tribocorrosion behaviors of AlFeCrNiMo high entropy alloy coatings and 304 stainless steel. *Materials Today Communications*, 24(February), 101261.
- Zhang, C., Gunes, O., Li, Y., Cui, X., Mohammadtaheri, M., Wen, S.-J., Wong, R., Yang, Q., & Kasap, S. (2019). The Effect of Substrate Biasing during DC Magnetron Sputtering on the Quality of VO₂ Thin Films and Their Insulator–Metal Transition Behavior. *Materials*, 12(13), 2160.
- Zhang, M., Zhou, X., Yu, X., & Li, J. (2017a). Surface & Coatings Technology Synthesis and characterization of refractory TiZrNbWMo high-entropy alloy coating by laser cladding. *Surface & Coatings Technology*, 311, 321–329.
- Zhang, M., Zhou, X., Yu, X., & Li, J. (2017b). Synthesis and characterization of refractory TiZrNbWMo high-entropy alloy coating by laser cladding. *Surface and Coatings Technology*, 311, 321–329.
- Zhang, X., Ma, S., Li, F., Yang, F., Liu, J., & Zhao, Q. (2013). Effects of substrate temperature on the growth orientation and optical properties of ZnO:Fe films synthesized via magnetron sputtering. *Journal of Alloys and Compounds*, 574, 149–154.
- Zhang, Y., Wang, D., & Wang, S. (2022). High-Entropy Alloys for Electrocatalysis: Design, Characterization, and Applications. *Small*, 18(7), 1–22.
- Zhang, Y., Zuo, T. T., Tang, Z., Gao, M. C., Dahmen, K. A., Liaw, P. K., & Lu, Z. P. (2014). Microstructures and properties

- of high-entropy alloys. *Progress in Materials Science*, 61(November 2013), 1–93.
- Zhao, F., Song, Z. X., Zhang, G. F., Hou, X. D., & Deng, D. W. (2013). Effects of substrate bias on structure and mechanical properties of AlCrTiWNbTa coatings. *Surface Engineering*, 29(10), 778–782.
- Zhao, S., Liu, C., Yang, J., Zhang, W., He, L., Zhang, R., Yang, H., Wang, J., Long, J., & Chang, H. (2021). Mechanical and high-temperature corrosion properties of AlTiCrNiTa high entropy alloy coating prepared by magnetron sputtering for accident-tolerant fuel cladding. *Surface and Coatings Technology*, 417(December 2020), 127228.
- Zhou, R., Chen, G., Liu, B., Wang, J., Han, L., & Liu, Y. (2018). Microstructures and wear behaviour of (FeCoCrNi)_{1-x}(WC)_x high entropy alloy composites. *International Journal of Refractory Metals and Hard Materials*, 75(April), 56–62.



© 2024 by the authors; licensee Growing Science, Canada. This is an open access article distributed under the terms and conditions of the Creative Commons Attribution (CC-BY) license (<http://creativecommons.org/licenses/by/4.0/>).